

Supplement of Atmos. Chem. Phys., 19, 7595–7608, 2019  
<https://doi.org/10.5194/acp-19-7595-2019-supplement>  
© Author(s) 2019. This work is distributed under  
the Creative Commons Attribution 4.0 License.



Atmospheric  
Chemistry  
and Physics  
Open Access  
EGU

*Supplement of*

## **New particle formation events observed at the King Sejong Station, Antarctic Peninsula – Part 2: Link with the oceanic biological activities**

**Eunho Jang et al.**

*Correspondence to:* Ki-Tae Park (ktpark@kopri.re.kr)

The copyright of individual parts of the supplement might differ from the CC BY 4.0 License.

## Calculation of the sea surface DMSP concentration

Several studies reported that DMSP and DMS were strongly linked to several environmental parameters such as solar radiation, sea-surface temperature, and mixing state of the sea surface (Vallina and Simo, 2007). *Gali et al.* (2015) developed a DMSP algorithm based on satellite-derived chlorophyll (to measure phytoplankton biomass) and the light exposure regime (to measure key environmental factors controlling DMSP production). In this algorithm, euphotic layer depth ( $Z_{eu}$ ) and mixed layer depth (MLD) dataset were applied to establish a mixing state of the sea surface (stratified vs. mixed water column), and the variability in modeled and measured DMSP was improved by adding sea-surface temperature and  $\log_{10}(Z_{eu}/MLD)$  as predictors for the stratified and mixed subsets in the proposed algorithm. Additionally, a sub-model based on particulate inorganic carbon (PIC) was developed to complement DMSP diagnosis in coccolithophore blooms, where satellite chlorophyll concentration may not be reliable. The database was divided into three subsets including ‘stratified water ( $Z_{eu}/MLD > 1$ )’, ‘mixed water ( $Z_{eu}/MLD < 1$ )’ and ‘undefined water ( $Z_{eu}$  or MLD is unavailable)’ based on the ratio between the euphotic layer depth ( $Z_{eu}$ ) and the mixed layer depth (MLD). The  $DMSP_t$  concentrations in stratified, mixed and undefined water were calculated using Equations (S1), (S2) and (S3), respectively:

$$\log_{10}DMSP_t = 1.70 + 1.14\log_{10}Chl_t + 0.44\log_{10}Chl_t^2 + 0.063SST - 0.0024SST^2 \quad (S1)$$

$$\log_{10}DMSP_t = 1.74 + 0.81\log_{10}Chl_t + 0.60\log_{10}(Z_{eu}/MLD) \quad (S2)$$

$$\log_{10}DMSP_t = -1.052 - 3.185\log_{10}PIC - 0.783(\log_{10}PIC)^2 \quad (S3)$$

The level-3 product of the Moderate Resolution Imaging Spectroradiometer on the Aqua (MODIS-Aqua) satellites was used for the chlorophyll concentration ( $Chl_t$ ), sea surface temperature at nighttime (SST) and the calcite concentration (PIC). The monthly mixed layer depth (MLD) was retrieved by Monthly Isopycnal and Mixed-layer Ocean Climatology (MIMOC) at a resolution of  $0.5^\circ$ . All of the MODIS-Aqua products at a resolution of 4 km were averaged onto a  $0.5^\circ$  interval grid of MIMOC climatology to run the  $DMSP_t$  algorithm. The euphotic layer depth ( $Z_{eu}$ ) was calculated using satellite-derived chlorophyll data as shown in Equation (S4) (Morel et al., 2007).

$$\log_{10}Z_{eu} = 1.524 - 0.436\log_{10}Chl_t - 0.0145(\log_{10}Chl_t)^2 + 0.0186(\log_{10}Chl_t)^3 \quad (S4)$$

## References

Gali, M., Devred, E., Levasseur, M., Royer, S.-J., and Babin, M.: A remote sensing algorithm for planktonic dimethylsulfoniopropionate (DMSP) and an analysis of global patterns, *Remote Sens. Environ.*, 171, 171–184, <https://doi.org/10.1016/j.rse.2015.10.012>, 2015.

Morel, A., Huot, Y., Gentili, B., Werdell, P. J., Hooker, S. B., and Franz, B. A.: Examining the consistency of products derived from various ocean color sensors in open ocean (Case 1) waters in the perspective of a multi-sensor approach, *Remote Sens. Environ.*, 111, 69–88, <https://doi.org/10.1016/j.rse.2007.03.012>, 2007.

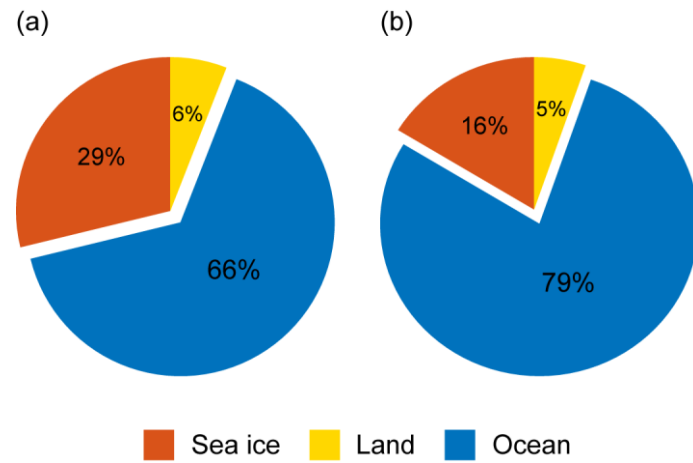
Vallina, S. M. and Simó, R.: Strong relationship between DMS and the solar radiation dose over the global surface ocean, *Science*, 315, 506–508, <https://doi.org/10.1126/science.1133680>, 2007.

**Table S1.** Monthly average, 1 standard deviation and 95% confidence interval of nanoparticles (2.5–10 nm in diameter, CN<sub>2.5-10</sub>) that originated from the Bellingshausen and Weddell Seas during the study period. A *t*-test was used to determine if there is a statistically significant difference between the means number concentration nanoparticles originated from the two selected ocean domains.

		Avg.	Std.	95% confidence interval*		<i>p</i> -value ( <i>t</i> -test)
				Upper bound	Lower bound	
Jan.	Weddell sea	332.0	920.7	196.3	782.4	0.0003
	Bellingshausen sea	835.9	2673.2	705.9	1004	
Feb.	Weddell sea	254.3	284.0	181.4	355.8	0.0010
	Bellingshausen sea	523.7	2130.7	417.2	695.4	
Mar.	Weddell sea	60.7	60.3	47.0	78.2	< 0.0001
	Bellingshausen sea	166.6	550.3	142.6	208.5	
Apr.	Weddell sea	70.0	103.6	53.9	96.4	0.0245
	Bellingshausen sea	100.9	272.4	87.7	126.6	
May	Weddell sea	89.6	74.5	75.2	108.4	< 0.0001
	Bellingshausen sea	45.2	56.2	41.0	50.9	
Jun.	Weddell sea	58.0	22.0	NaN**	NaN	NaN
	Bellingshausen sea	57.7	62.1	52.7	64.1	
Jul.	Weddell sea	22.9	17.9	15.1	35.1	0.0031
	Bellingshausen sea	42.8	56.8	36.8	51.6	
Aug.	Weddell sea	-	-	NaN	NaN	NaN
	Bellingshausen sea	58.3	78.6	47.5	73.6	
Sep.	Weddell sea	3.7	-	NaN	NaN	NaN
	Bellingshausen sea	97.9	85.9	91.0	105.5	
Oct.	Weddell sea	193.1	160.5	NaN	NaN	NaN
	Bellingshausen sea	129.0	405.1	110.3	197.7	
Nov.	Weddell sea	88.0	61.0	74.3	107.4	< 0.0001
	Bellingshausen sea	176.7	331.9	154.0	214.3	
Dec.	Weddell sea	200.5	380.5	56.5	499.9	0.2111
	Bellingshausen sea	343.0	1138.8	277.6	449.0	

5 \*confidence interval was estimated by bootstrap method that was calculated from 10,000 subsamples generated by random sampling with replacement from monthly CN<sub>2.5-10</sub> data.

\*\*number of monthly CN<sub>2.5-10</sub> data <10 was excluded from the bootstrap and *t*-test.



5 **Figure S1:** Percentage of the hourly trajectory points that passed over the three major areas surrounding the observation site including sea-ice (red), land (yellow) and ocean (blue) to the total number of hourly trajectory points in the 2-day air-mass trajectory during (a) the overall period (from January to December) and (b) the austral summer period (December, January and February) between March 2009 and November 2016.

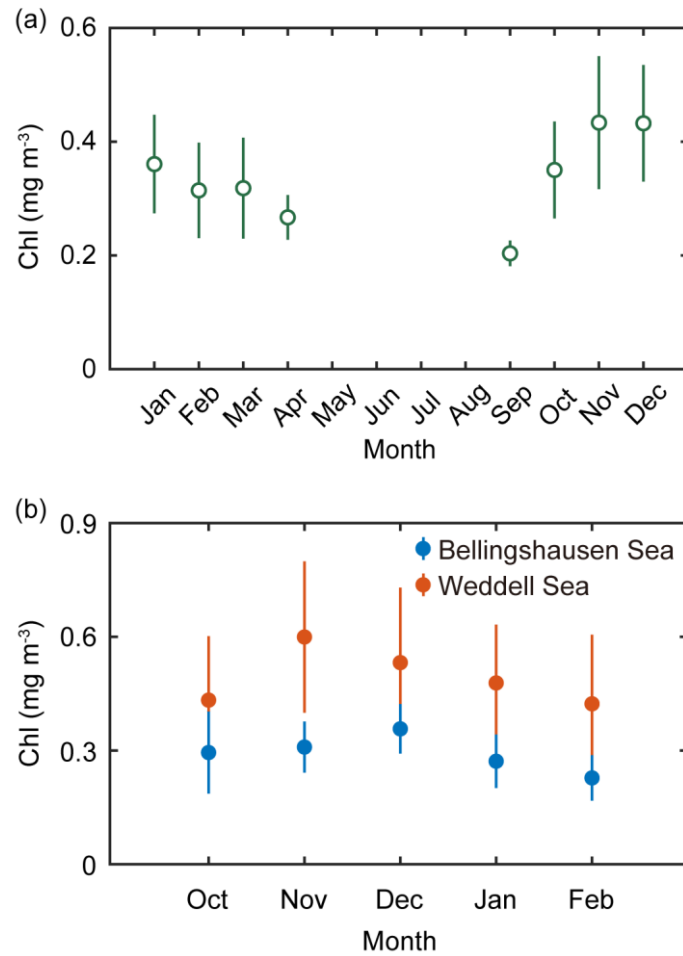


**Figure S2:** (a) Monthly mean chlorophyll concentration around the observation site between 2009 and 2016 (55°S–65°S, 40°W–80°W). (b) Monthly mean chlorophyll concentration for the two selected ocean domains including the Weddell (red symbols; 55°S–65°S, 40°W–60°W) and Bellingshausen (blue symbols; 55°S–65°S, 60°W–80°W) seas during the phytoplankton bloom period (October–February). Note that the monthly mean chlorophyll concentration was not available from May to August due to insufficient satellite-derived values (less than 10%) during the austral winter period.

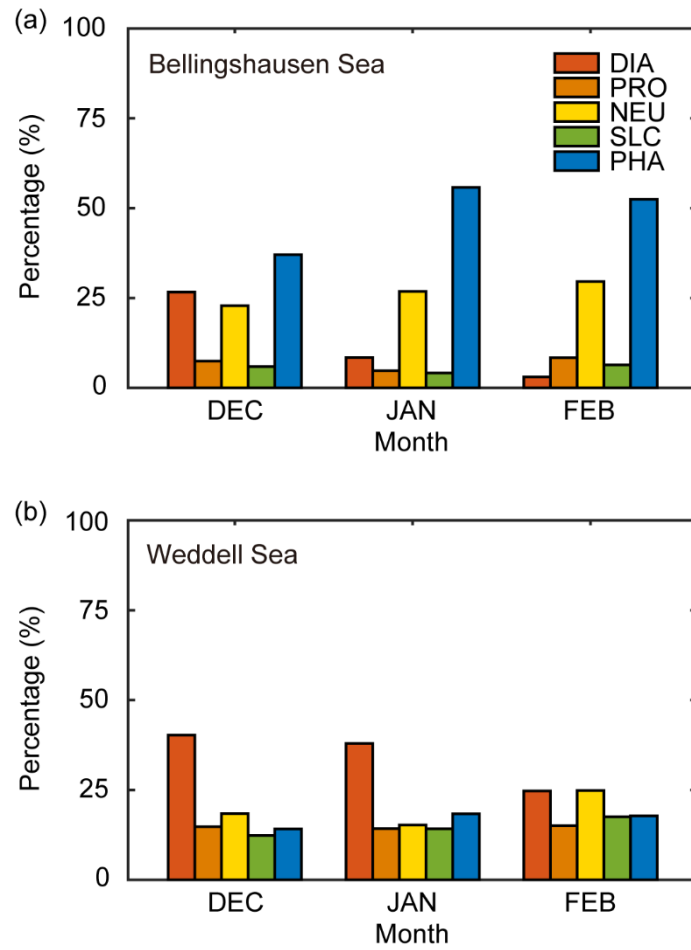


**Figure S3:** The percentage of the dominant phytoplankton groups in the two ocean domains including (a) the Bellingshausen and (b) Weddell seas estimated using the PHYSAT method with the climatology map obtained from SeaWiFS archive during the austral summer period.

5

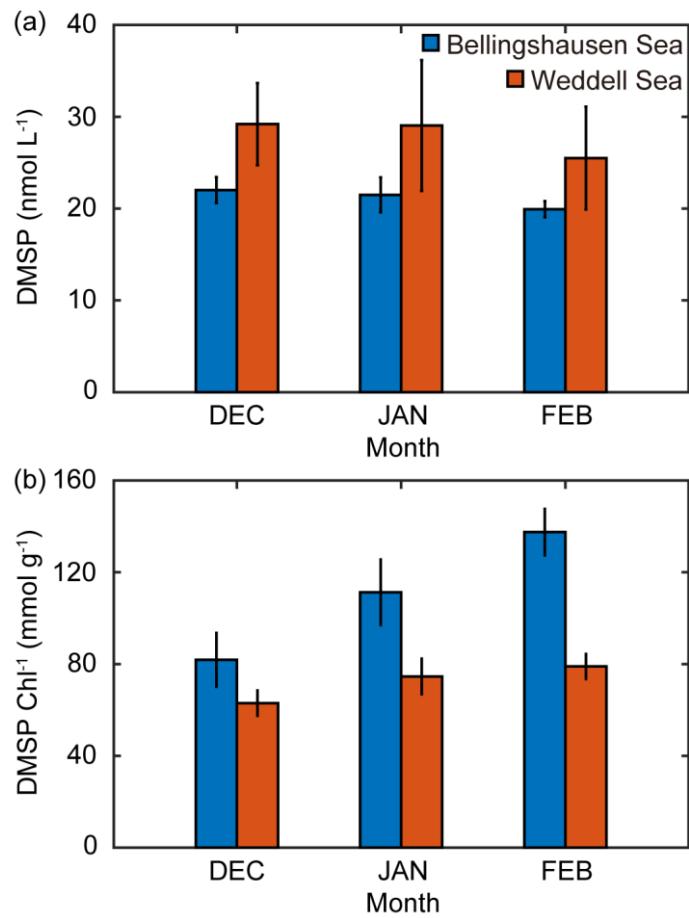


**Figure S4:** (a) Monthly mean DMSP concentration and (b) monthly mean DMSP-to-chlorophyll ratio in the Bellingshausen (blue bars) and Weddell (red bars) Seas during the austral summer period between March 2009 and November 2016.

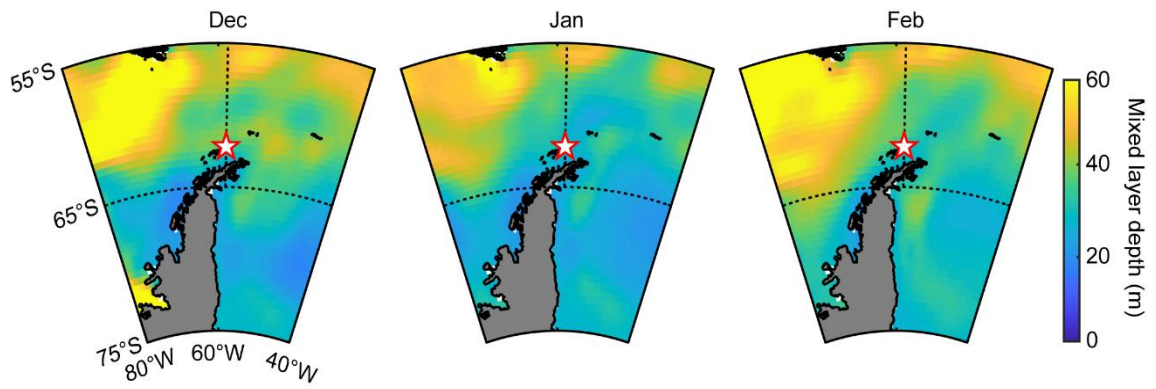


**Figure S5:** Mixed layer depth retrieved using the Monthly Isopycnal and Mixed-layer Ocean Climatology (MIMOC) during the austral summer period surrounding King Sejong Station (red star symbol).

5